EXAFS Studies of Binuclear Iron Proteins: Hemerythrin and Ribonucleotide Reductase

Robert C. Scarrow,[†] Michael J. Maroney,[†] Sharon M. Palmer,[†] Lawrence Que, Jr.,*[†] A. Lawrence Roe,[†] Scott P. Salowe,[‡] and JoAnne Stubbe[‡]

Contribution from the Department of Chemistry, University of Minnesota, Minneapolis, Minnesota 55455, and Department of Biochemistry, College of Agriculture and Life Sciences, University of Wisconsin—Madison, Madison, Wisconsin 53706. *Received January 5, 1987*

Abstract: The iron K-edge EXAFS spectra of methemerythrin azide (metHrN_3), semimethemerythrin azide (semimetHrN_3), and the B_2 subunit of ribonucleotide reductase from *Escherichia coli* (RRB_2) have been analyzed and compared with those of several binuclear and tetranuclear model compounds. The synthetic complexes include compounds with hydroxo and oxo bridges and several with the triply bridged diiron core similar to that found in metHrN_3. The analysis allows the determination of the presence of a short Fe–O distance among longer Fe–O(N) distances and the estimation of average bond lengths and the second-shell Fe–Fe distance with esd's of 0.015 and 0.02 Å, respectively. Both metHrN_3 and RRB_2 exhibit short Fe–O (1.79 and 1.78 Å, respectively) bonds and similar Fe–Fe (3.19 and 3.22 Å, respectively) distances, suggesting that the metal sites of the two proteins share the same (μ-oxo)bis(μ-carboxylato)diiron core. However, the average bond length for the remaining ligands in the first coordination sphere of RRB_2 is 0.07 Å shorter than that of metHrN_3. This suggests that at least one histidine per iron in metHrN_3 is replaced by an oxyanion ligand in RRB_2, since Fe–O bonds are significantly shorter than Fe–N bonds in high-spin ferric complexes. The analysis for semimetHrN_3 indicates that the short Fe–O bonds found in metHrN_3 have significantly lengthened in semimetHrN_3. The Fe–Fe distance increases to 3.46 Å, while the average bond length for the other ligands increases by only 0.01 Å. These results are interpreted in terms of a localized mixed valent Fe(III)–Fe(II) complex bridged by hydroxide and two carboxylates, consistent with previously reported NMR and Raman data.

Hemerythrin and ribonucleotide reductase from *Escherichia coli* are members of an emerging class of metalloproteins with binuclear iron sites. Hemerythrin is a dioxygen carrier in marine sipunculids,[1] while ribonucleotide reductase catalyzes the conversion of nucleoside diphosphates to deoxynucleoside diphosphates.[2] The active sites of hemerythrin (Hr) in its met and oxy states[1] and the B_2 subunit of ribonucleotide reductase (RRB_2) from *E. coli*[2] share several common characteristics. Both active sites feature binuclear ferric centers that are strongly coupled antiferromagnetically ($-J \approx 100$ cm^{-1}),[3,4] and both have similar visible and resonance Raman spectra;[5,6] this has led to the suggestion that the two proteins may have similar active site structures.[7]

X-ray crystallography and a variety of spectroscopic methods (including EXAFS) have established that the iron centers in metHr, metHrX, and oxyHr are bridged by an oxo group and two carboxylates.[1] Histidines occupy five of the six remaining coordination positions, and the sixth site is vacant in metHr and occupied by the anion in metHrX and by dioxygen in oxyHr. Semimethemerythrin azide (SemimetHrN_3) is formed by the addition of azide to either the product of one-electron reduction of metHr or the product of one-electron oxidation of deoxyHr. Raman[8] and NMR[9] studies show valence localization in this mixed-valence complex with azide bound to the ferric center. NMR studies further demonstrate that the antiferromagnetic coupling between the iron centers is substantially diminished ($J \approx -20$ cm^{-1}) relative to that in metHr and metHrX, suggesting the possibilities of structural changes in the bridging core structure.[9]

Little is known of the coordination chemistry of the binuclear iron site of ribonucleotide reductase from *E. coli*, aside from the participation of the oxo bridge. This site has been shown to be involved in the generation and the stabilization of the catalytically important tyrosyl cation radical.[2] Reduction of the radical by hydroxyurea inactivates RRB_2, but the binuclear iron site is retained.

We have conducted an EXAFS comparison of methemerythrin azide (metHrN_3), semimetHrN_3, and RRB_2 in order to determine whether the (μ-oxo)bis(μ-carboxylato)diiron core is a common structural feature found in this class of proteins. Based on EXAFS data for a number of crystallographically characterized iron complexes with coordination environments similar to that of Hr, an analysis protocol has been developed to determine the presence of a short (1.8-Å) Fe–O bond amidst longer iron–ligand distances and to estimate iron–iron distances. Some results of this work have been communicated recently.[10]

Experimental Section

Sample Preparation and Data Collection. The crystallographically characterized model complexes used in this study are shown in Figure 1, with the exception of $[(TPP)Fe]_2O$ (**2**).[11] Compounds **1–6** were synthesized and crystallized in our laboratory according to published procedures.[7,12-15] We gratefully acknowledge the generous gifts of

[†] University of Minnesota.
[‡] University of Wisconsin—Madison.

(1) Sanders-Loehr, J.; Loehr, T. M. *Adv. Inorg. Biochem.* **1979**, *1*, 235–252. Wilkins, R. G.; Harrington, P. C. *Adv. Inorg. Biochem.* **1983**, *5*, 51–85. Klotz, I. M.; Kurtz, D. M., Jr. *Acc. Chem. Res.* **1984**, *17*, 16–22.
(2) Sjöberg, B.-M.; Graslund, A. *Adv. Inorg. Biochem.* **1983**, *5*, 87–110.
(3) Dawson, J. W.; Gray, H. B.; Hoenig, H. E.; Rossman, G. R.; Schredder, J. M.; Wang, R. H. *Biochemistry* **1972**, *11*, 461–465.
(4) Petersson, L.; Graslund, A.; Ehrenberg, A.; Sjöberg, B.-M.; Reichard, P. J. *J. Biol. Chem.* **1980**, *255*, 6706–6712.
(5) Shiemke, A. K.; Loehr, T. M.; Sanders-Loehr, J. *J. Am. Chem. Soc.* **1986**, *108*, 2437–2443 and references therein.
(6) Sjöberg, B.-M.; Loehr, T. M.; Sanders-Loehr, J. *Biochemistry* **1982**, *21*, 96–102.
(7) Armstrong, W. H.; Spool, A.; Papaefthymiou, G. C.; Frankel, R. B.; Lippard, S. J. *J. Am. Chem. Soc.* **1984**, *106*, 3653–3667.
(8) Irwin, M. J.; Duff, L. J.; Shriver, D. F.; Klotz, I. M. *Arch. Biochem. Biophys.* **1983**, *224*, 473–478.
(9) Maroney, M. J.; Kurtz, D. M., Jr.; Nocek, J. M.; Pearce, L. L.; Que, L., Jr. *J. Am. Chem. Soc.* **1986**, *108*, 6871–6879.
(10) Scarrow, R. C.; Maroney, M. J.; Palmer, S. M.; Que, L., Jr. *J. Am. Chem. Soc.* **1986**, *108*, 6832–6834.
(11) Chemical abbreviations used: acac, 2,4-pentanedione; acacen, 2,11-dihydroxy-4,9-dimethyl-5,8-diazadodeca-2,4,8,10-tetraene; HB($pz)_3$, hydrotris(pyrazolyl)borate; HXTA, *N,N'*-(2-hydroxy-5-methyl-1,3-xylylene)bis[*N*-(carboxymethyl)glycine]; Me_3tacn, 1,4,7-trimethyl-1,4,7-triazacyclononane; OAc, acetate; tacn, 1,4,7-triazacyclononane; TPP, *meso*-tetraphenylporphyrin.
(12) Iball, J.; Morgan, C. H. *Acta. Crystallogr.* **1967**, *23*, 239–244.
(13) Hoffman, A. B.; Collins, D. M.; Day, V. W.; Fleischer, E. B.; Srivastava, T. S.; Hoard, J. L. *J. Am. Chem. Soc.* **1972**, *94*, 3620–3626.
(14) Murch, B. P.; Boyle, P. D.; Que, L., Jr. *J. Am. Chem. Soc.* **1985**, *107*, 6725–6729.
(15) Armstrong, W. H.; Lippard, S. J. *J. Am. Chem. Soc.* **1984**, *106*, 4632–4633.

0002-7863/87/1509-7857$01.50/0

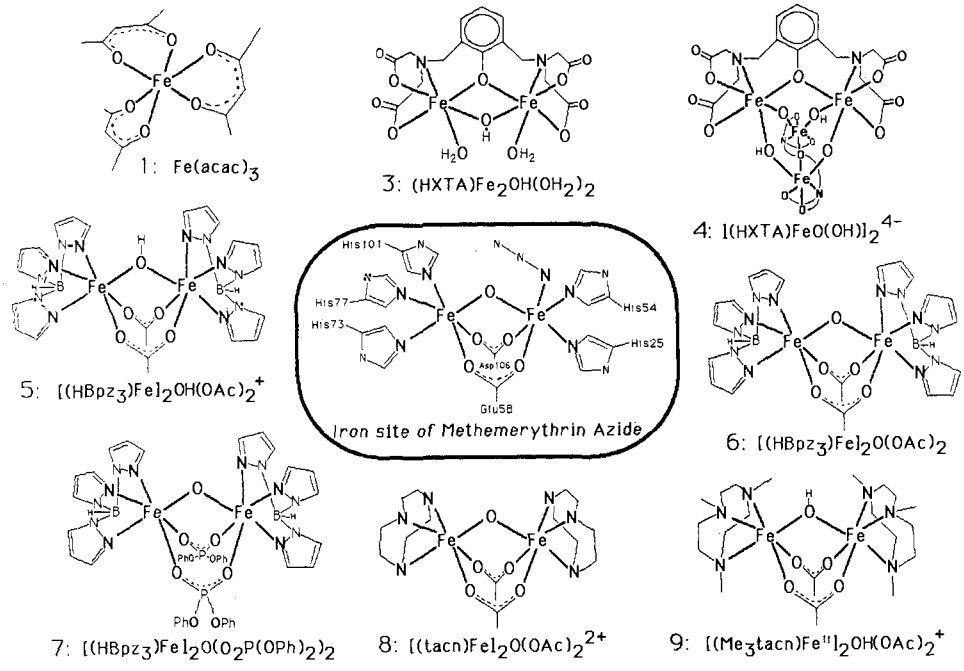

Figure 1. Model complexes **1** and **3–9**. Also shown is the structure of the binuclear iron core of metHrN$_3$.

compound **7**[16] by Prof. S. J. Lippard and compounds **8**[17] and **9**[18] by Prof. K. Wieghardt.

MetHrN$_3$ was prepared by adding a 10-fold excess of NaN$_3$ to 4 mL of 1.7 mM metHr (from *Phascolopsis gouldii*, prepared as previously described[9]) in 50 mM phosphate buffer (pH 7.5) containing 50 mM NaClO$_4$. Upon complex formation, the buffer was changed to 20 mM Tris perchlorate buffer (pH 8.0), and the solution was concentrated to yield the EXAFS sample (16 mM based on $A_{446\ nm}$[19]). The optical purity index of metHrN$_3$ ($A_{446\ nm}/A_{326\ nm}$) was 0.52 before and after measurement of the EXAFS. SemimetHrN$_3$ in 20 mM Tris perchlorate buffer (pH 8.0) was prepared from metHr under anaerobic conditions by successive additions of 1 equiv of dithionite and 13 equiv of NaN$_3$. The resulting solution was concentrated to 7 mM, based on EPR integration,[20] which was unchanged after exposure to the X-ray beam.

RRB$_2$ was isolated from *E. coli* strain N6405/pSPS2, a heat-inducible overproducer.[21] Protein concentration was 2.8 mM in 50 mM Tris acetate buffer (pH 7.6) containing 0.1 mM Na$_2$EDTA. The UV/vis spectra and enzyme activity (3.4 μmol/min per mg) were monitored before and after beam exposure; neither changed significantly. EXAFS spectra of two samples of RRB$_2$ were averaged for the analyses reported in this paper. In addition, the EXAFS spectrum of a single sample of RRB$_2$ with added hydroxyurea was measured. The UV/vis spectrum of this sample was unchanged after X-ray exposure.

Protein samples in buffers containing 20% ethylene glycol (to inhibit ice crystal formation) were frozen in 3 × 3 × 20 mm notches in gold-plated copper sample holders. The sample holders were then attached to a liquid nitrogen cryostat (Janis) in an evacuated chamber with X-ray beam ports made of 3-mil Mylar. The model complexes were studied as powders at room temperature.

X-ray absorption spectra (XAS) were collected between 6.9 and 7.9 keV at stations C-1 and C-2 of the Cornell High Energy Synchrotron Source (CHESS). The monochromator was calibrated by using the 7113.0-eV 1s → 3d peak in the XAS spectrum of [Et$_4$N][FeCl$_4$] (suspended in Duco cement). The energy of this peak was determined relative to the first inflection in the K-edge spectrum of iron foil at 7111.2 eV.[22] The XAS (A_{exp}) was determined from the counts observed from the incident (C_0) and either transmission (C_t) or fluorescence (C_f) ionization detectors. EXAFS of model complexes were generally obtained by transmission measurements, and $A_{exp} = \ln (C_0/C_t)$. Fluorescence measurements ($A_{exp} = C_f/C_0$) were used for **2**, **7**, one sample of **1**, and for the protein samples. A large solid-angle fluorescence detector was used with a Mn filter and Soller slits.[23]

Data Analysis. The treatment of the raw EXAFS data (A_{exp}) to yield χ is discussed at length in review articles.[24,25] EXAFS is defined as $\chi = (\mu_{Fe}^s - \mu_{Fe}^0)/\mu_{Fe}^0$; it is the fractional difference in the iron K-shell absorption of the sample (μ_{Fe}^s) compared with monoatomic iron gas (μ_{Fe}^0, from tabulated coefficients[26]). As shown in Table S1 (supplementary material), $\mu_{Fe}^s = aA_{exp} - b$, where a and b are functions of energy, so $\chi = [aA_{exp} - (b + \mu_{Fe}^0)]/\mu_{Fe}^0$. We use a three-region cubic spline function to approximate $b + \mu_{Fe}^0$. The magnitude of a is determined from the K-edge jump in A_{exp}. For transmission data, a is constant, but a varies with energy for fluorescence data. The variation in a is due to the energy dependence of the X-ray penetration depth (for thick samples such as ours), the detector efficiencies, and absorbance by air and cryostat windows. The calculations of these effects are shown in Table S1. The effects are significant; a at 7900 eV was calculated to be 70% of that at 7125 eV. The extraction of χ from A_{exp} employed a modification of the program EXAPLT.[27]

Least-squares fits were used to determine iron–ligand distances and details of the iron coordination using single-scattering EXAFS theory and theoretical scattering functions, as reviewed elsewhere[25,28]

$$\chi_c = \sum_{\text{shells}} nA[f(k')]k'^{-1}r^{-2}e^{-2\sigma k'^2} \sin (2k'r + \alpha(k')) \qquad (1)$$

where

$$k' = [4\pi m_e(E - (7125\ \text{eV} + \Delta E))/h]^{1/2} \qquad (2)$$

Each shell consists of n atoms at distance $r \pm \sigma$ from the iron atom. The amplitude reduction factor (A) and the shell-specific edge shift (ΔE) are empirical parameters that partially compensate for imperfections in the theoretical functions f and α.[29]

(16) Armstrong, W. H.; Lippard, S. J. *J. Am. Chem. Soc.* **1985**, *107*, 3730–3731.
(17) Wieghardt, K.; Pohl, K.; Gebert, W. *Angew. Chem., Int. Ed. Engl.* **1983**, *22*, 727.
(18) Chaudhuri, P.; Wieghardt, K.; Nuber, B.; Weiss, J. *Angew. Chem., Int. Ed. Engl.* **1985**, *24*, 778–779.
(19) Garbett, K.; Darnall, D. W.; Klotz, I. M.; Williams, R. J. P. *Arch. Biochem. Biophys.* **1969**, *103*, 419–434.
(20) The EPR integrations were performed in the laboratory of Prof. D. M. Kurtz according to procedures in the following paper: Lukat, G. S.; Kurtz, D. M., Jr. *Biochemistry* **1985**, *24*, 3464–3472.
(21) Salowe, S. P.; Stubbe, J. *J. Bacteriol.* **1986**, *165*, 363–366.
(22) Bearden, J. A.; Burr, A. F. *Rev. Mod. Phys.* **1967**, *39*, 78–124.
(23) Stern, E. A.; Heald, S. M. *Rev. Sci. Instrum.* **1979**, *50*, 1579–1582.
(24) Cramer, S. P.; Hodgson, K. O. *Prog. Inorg. Chem.* **1979**, *25*, 1–39.
(25) Scott, R. A. *Methods Enzymol.* **1985**, *117*, 414–459.
(26) McMaster, W. H.; Kerr Del Grande, N.; Mallett, J. H.; Hubbell, J. H. *Compilation of X-ray Cross Sections*; National Technical Information Service, U.S. Chamber of Commerce: Springfield, VA, 1969; UCRL-50174 Sec. II, Rev. 1.
(27) We are grateful to Dr. C. Marcus for providing us with a copy of his EXAPLT.
(28) Teo, B. K. In *EXAFS Spectroscopy, Techniques and Applications*; Teo, B.-K., Joy, D. C., Eds.; Plenum: New York, 1981; pp 13–58.
(29) Teo, B. K.; Lee, P. A. *J. Am. Chem. Soc.* **1979**, *101*, 2815–2832.

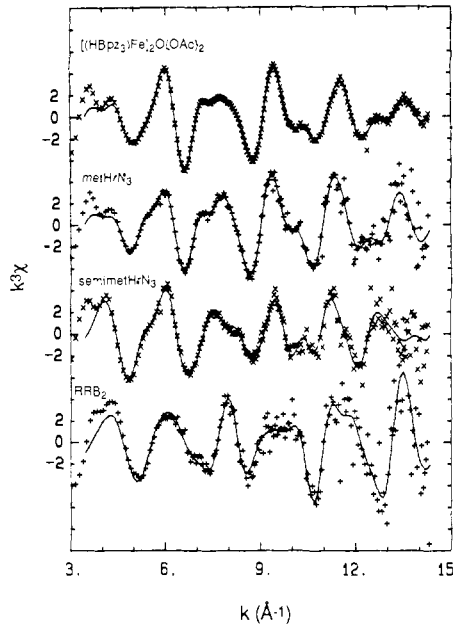

Figure 2. EXAFS spectra ($k^3\chi$) of (top to bottom) **6**, metHrN$_3$, semimetHrN$_3$, and RRB$_2$. The dashed lines are the spectra with noise removed by Fourier filtering. The forward transform and back-transform limits are 3.5–14.3 Å^{-1} and 1.1–4.5 Å, respectively.

Least-squares refinements used the Newton–Gauss algorithm and used locally developed software. The refinements reported were on $k^3\chi$, and the function minimized was $R \equiv \{\sum k^6(\chi_c - \chi)^2/n\}^{1/2}$, where the sum is over the n data points between 4 and 14 Å^{-1}. The refinement program allows Fourier filtering of both $k^3\chi$ and $k^3\chi_c$ in order to isolate contributions from specific coordination spheres.[25,30] The program can also use unfiltered data to simultaneously refine EXAFS parameters and cubic spline parameters for the background function $b + \mu_{Fe}{}^0$.[31] Such "multishell" refinements eliminate large peaks below $r' = 1$ Å in the Fourier transforms of $k^3\chi$ (and of the difference spectra $k^3(\chi_c - \chi)$).[32]

Results and Discussion

The nine model complexes used for the EXAFS analysis [except [(TPP)Fe]$_2$O (**2**)] are illustrated in Figure 1 along with the structure of metHrN$_3$ determined by X-ray crystallography.[8,33] All except **9** are ferric complexes. The complexes **5–9** exhibit the triply bridged diiron core structure of hemerythrin; **5** and **9** have hydroxo bridges and **6–8** have oxo bridges. Compound **3** is a hydroxo- and phenoxo-bridged diiron complex, and **4** is a tetranuclear complex with an Fe$_4$O$_6$ core containing two oxo, two hydroxo, and two phenoxo bridging ligands. Analysis of EXAFS spectra of these compounds yielded parameters used in subsequent fits of the EXAFS spectra of metHrN$_3$, semimetHrN$_3$, and RRB$_2$ in its native and radical-free forms.

The EXAFS spectra of **6**, metHrN$_3$, semimetHrN$_3$, and RRB$_2$ are compared in Figure 2. The magnitudes of the Fourier transform of $k^3\chi$ for several of the small inorganic compounds and proteins are compared in Figure 3. Peaks in the Fourier transform at $r' = 1.6$–1.8 Å are due to bond lengths of 2.0–2.2 Å and the peaks at $r' \approx 2.8$ Å are due to scattering from second coordination sphere atoms. The short Fe–μ-oxo bonds of **2**, **6**, and metHrN$_3$ do not give separate peaks in the transform; counterintuitively, the 1.6-Å peak in the transform appears to be narrowed by the presence of the short Fe–O bond.

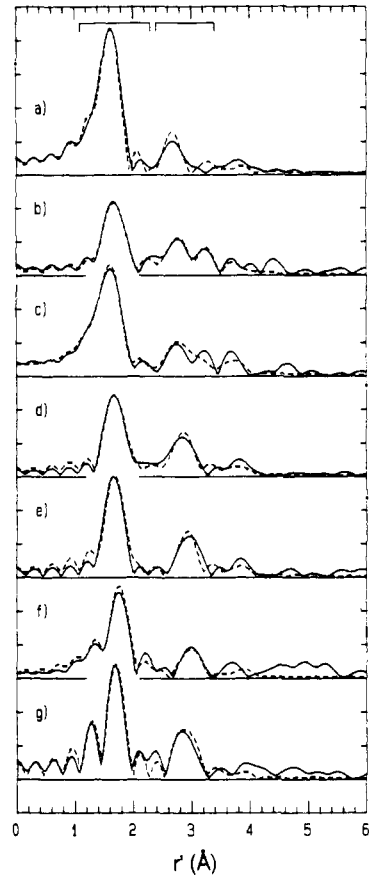

Figure 3. Magnitude of Fourier transforms of $k^3\chi$ for several protein samples and model compounds. Key: (a) **1**, (b) **2**, (c) **5**, (d) **6**, (e) metHrN$_3$, (f) semimetHrN$_3$, (g) RRB$_2$. Dashed lines indicate the Fourier transforms of the multishell fits to the data.

Development of Analysis Protocol Using Model Complexes. Using the model complexes **1–9**, we have developed a restricted-fit protocol to obtain interatomic distances from the $k^3\chi$ data. EXAFS analyses of several of these compounds (**5–8**) have been previously reported.[34] These analyses, as well as earlier EXAFS analyses of metHrN$_3$ (see below) used empirical amplitude and phase functions (f and α in eq 1) derived from analysis of model compounds. In contrast, our analyses use the theoretical functions of Teo and Lee, with two empirical parameters (A and ΔE) per shell.[29] For **5–8**, both methods yield similar bond lengths and Fe–Fe separations.

Our analysis protocol uses known crystal structures to determine for each shell A, ΔE, and, for shells where n is unknown, σ^2. This is similar to the "fine adjustment based on models" (FABM) method,[35] but has been devised for coordination environments that have more than one M–X distance per coordination sphere. This leaves two parameters per shell (r and σ^2 or n) to be refined, which eliminates large correlations—between r and ΔE and between nA and σ^2—that are observed when four parameters per shell are refined (BFBT or "best fit based on theory" refinements[35]). Although BFBT always fits the data better due to the increased number of refined parameters, the restricted fits give values for interatomic distances more consistent with the values known from crystal structures of the model compounds. For this reason we

(30) The $k^3\chi$ data between $k = 3.5$ and 14.3 Å was first multiplied by a "5% windowing function" (=sin [minimum$\{\pi/2, (k - 3.5$ Å$^{-1})/x, (14.3$ Å$^{-1} - k)/x\}$], where $x = 0.34$ Å^{-1}) and then Fourier transformed to r' space. The back-transform was over various limits (as described in the text and in table captions) and did not employ a windowing function. Because the calculated EXAFS is Fourier transformed in exactly the same manner, the transform limits and the presence or absence of windowing do not critically affect the results.

(31) The function $b + \mu_{Fe}{}^0$ is fit to a three-region cubic spline with spline points at 7405 and 7645 eV. Correlation coefficients as high as 0.7 were observed between base-line and first-sphere structural parameters.

(32) These peaks can sometimes be eliminated by careful choice of curve-fitting limits for an initial spline fit of A_{exp} (for instance, using 7137 eV instead of 7140 eV as the lower limit might make a large difference in the low r' region for a particular data set);[25] however, simultaneous refinements provide a more objective method of removing the low r' base-line error.

(33) Stenkamp, R. E.; Sieker, L. C.; Jensen, L. H. *Acta Crystallogr. B: Struct. Sci.* **1983**, *B39*, 697–703. Stenkamp, R. E.; Sieker, L. C.; Jensen, L. H. *J. Am. Chem. Soc.* **1984**, *106*, 618–622.

(34) Hedman, B.; Co., M. S.; Armstrong, W. H.; Hodgson, K. O.; Lippard, S. J. *Inorg. Chem.* **1986**, *25*, 3708–3711.

(35) Teo, B. K.; Antonio, M. R.; Averill, B. A. *J. Am. Chem. Soc.* **1983**, *105*, 3751–3762.

Table I. Results from One- and Two-Shell Restricted Fits of First-Coordination-Sphere Fourier-Filtered EXAFS Spectra of Model Complexes and Proteins[a]

		shell 1s[b]			shell 1[c]			quality of fit		
no.	sample	n	r	σ^2	n	r	σ^2	R	Δr_{1s}	Δr_1
1T	$Fe(acac)_3$				6	1.998	27	0.56		+6
1F	$Fe(acac)_3$ (fluor. detn)				6	2.003	30	0.50		+11
1C	$Fe(acac)_3$ (77 K)				6	1.991	12	0.73		
2	$(FeTPP)_2O$				*5*	*2.093*	*38*	*1.15*		*+71*
		1	1.757	5	4	2.090	30	0.21	−6	+3
3	$(HXTA)Fe_2OH(OH_2)_2$				6	2.004	46	0.78		−20
4	$[(HXTA)Fe_2O(OH)]_2^{4-}$				*6*	*2.123*	*263*	*0.85*		*+71*
		1	1.791	14	5	2.104	108	0.43	0	0
5	$[(HB(pz)_3)Fe]_2OH(OAc)_2^+$	*1*	*1.919*	*27*	*5*	*2.034*	*−2*	*0.42*	*−36*	*−27*
					6	2.020	13	0.47		−23
6	$[(HB(pz)_3)Fe]_2O(OAc)_2$				*6*	*2.132*	*36*	*1.05*		*+72*
		1	1.783	−1	5	2.120	18	0.22	−1	+4
7	$[HB(pz)_3Fe]_2O(O_2P(OPh)_2)_2$				*6*	*2.126*	*28*	*1.16*		*+64*
		1	1.783	1	5	2.115	11	0.27	−25	+3
8	$[(tacn)Fe]_2O(OAc)_2^{2+}$				*6*	*2.151*	*82*	*0.99*		*+88*
		1	1.785	7	5	2.134	48	0.38	+1	+15
9	$[(Me_3tacn)Fe]_2OH(OAc)_2$				6	2.224	310	0.29		+38
10	$metHrN_3$				*6*	*2.137*	*13*	*1.61*		
		1	1.787	−22	5	2.129	3	0.45		
11	$semimetHrN_3$				*6*	*2.138*	*34*	*0.66*		
		1	*1.867*	45	*5*	*2.134*	*3*	*0.35*		
		0.5	1.863	−13	5.5	2.132	19	0.32		
12	RRB_2				*6*	*2.077*	*33*	*1.51*		
		2	*1.785*	*21*	*4*	*2.056*	*−7*	*0.88*		
		1	1.784	−26	5	2.060	16	0.30		
13	RRB_2 + hydroxyurea				6	2.074	62	1.37		
		1	1.778	−23	5	2.058	30	0.41		

[a] The $k^3\chi$ data was Fourier transformed over k = 3.5–14.3 Å^{-1} and back-transformed over 1.1–2.3 Å. Units are Å and pm^2 for r and σ^2, respectively. The Δr values are $(r_{EXAFS} - r_{cryst}) \times 10^3$ Å^{-1}, where r_{cryst} is an appropriate average distance from the published crystal structure. Numbers in italics are from alternate, less favored fits. [b] Shell 1s modeled as oxygen. [c] Shell 1 for complexes with mixed O/N coordination were modeled as oxygen and nitrogen subshells with known n_N and n_O. For proteins n_N was set to 3. The subshells were constrained so that $r_N = r_O + 0.12$ Å and $\sigma^2_N = \sigma^2_O$. The reported $n = n_N + n_O$ and $r = (n_N r_N + n_O r_O)/n$.

report results from the restricted fits in Table I. For comparison, BFBT fits are shown in Table S2 (supplementary material).

First Coordination Sphere. Fourier-filtered EXAFS spectra were used in initial analysis, including determination of A and ΔE, since these allowed examination of one coordination sphere at a time. To isolate the first coordination sphere, back-transform limits of 1.1–2.3 Å were used (see Figure 3). One- and two-shell BFBT fits for **1–9** are shown in Table S2. One-shell BFBT analyses gave very similar results for EXAFS from two samples of $Fe(acac)_3$, one examined by monitoring transmission and the other by monitoring fluorescence. The refined amplitude reduction factor (A = 0.44) was assumed for first coordination sphere O and N scatterers in all subsequent analyses. Amplitude reduction factors are typically ca. 0.5.[29,35]

Modeling nitrogen atoms as oxygen atoms causes a systematic decrease in the apparent values of both n and r, due to differences in the theoretical amplitude and phase functions for nitrogen and oxygen. The decrease in r is ca. 0.025 Å. Thus, we have explicitly included the mixed N/O ligation in modeling shell 1. However, other than the short iron–μ-oxo bonds, the iron–ligand bond lengths are too close in length to be resolved.[36] In our restricted fits, we have modeled shell 1 as a subshell of n_O oxygen atoms and another subshell of n_N nitrogen atoms, but with constraints such that $\sigma^2_N = \sigma^2_O$ and $r_N = r_O + 0.12$ Å. The latter constraint is based on the observation that Fe–N bonds are longer than Fe–O (excluding Fe–μ-oxo) bonds in crystal structures of **3–9** When mixed O/N shells are employed, we report the refined average distance, $r_{av} = (n_N r_N + n_O r_O)/(n_N + n_O)$.

For the first sphere, we fix values of n in the restricted fits, because of the inaccuracies in refined n values caused by correlation with σ^2 in BFBT fits (see Table S2). We choose not to fix σ^2 (as in the FABM method), because σ^2 is not known for **1–9** and because we expect σ^2 to be different for the protein samples. Since iron(III) in coordination compounds (including iron proteins) is usually 6-coordinate, we fix n_1 or $n_{1s} + n_1$ to be 6 (except for **2**, where $n_{1s} + n_1 = 5$, as known from the structure). For chemically similar compounds, first-sphere O/N shells are expected to have similar values of ΔE, and an appropriate value can be determined by analyzing the EXAFS of the model complexes (see Figure S1).[35] A ΔE value of 9 eV was used in subsequent restricted fits. The values of r and σ^2 refined by this method for the first-shell Fourier-filtered EXAFS spectra are given in Table I. For those compounds with a μ-oxo bridge, better fits (R decreased by 40–80%) were obtained with a two-shell fit. In contrast, adding a 1.8-Å Fe–O bond to the refinement model for compounds without μ-oxo bridges did not yield a least-squares minimum, except for **5** where r_{1s} refined to 1.92 Å. In this case the 10% decrease in R for the two-shell fit relative to the one-shell fit is probably too small to justify the additional variables in the former.

Second Coordination Sphere. The EXAFS spectrum was Fourier filtered using back-transform limits of 2.4–3.4 Å for analysis of the second coordination sphere of the binuclear iron complexes, which contains many more atoms than the first and has a greater diversity of distances (see Figure S3, supplementary material). Most of the second-sphere atoms are carbon atoms and a few other light (B, N, O) scatterers and, for binuclear iron centers, one iron–iron distance of 3.0–3.6 Å. In many of the model compounds, five to eight carbon (and/or nitrogen) atoms are at almost the same approximately 3-Å distance from each iron atom. This number of low Z scatterers will contribute approximately as much to the EXAFS as the single iron scatterer, although the contributions from C and N atoms should attenuate rapidly with increasing k.[28,29] In the model compounds there are also Fe–(O/C) distances of 3.2–3.4 Å, but the shells that include these atoms have fewer (one to three) scatterer atoms/iron and are expected to contribute relatively less to the EXAFS because these atoms are three bonds, rather than two, from the iron, and hence probably have higher values of σ^2.

We find that the second-sphere EXAFS of model compounds **3–6**, **8**, and **9** can be satisfactorily fit by a two-shell fit—one carbon

(36) Attempts to divide shell 1 into nitrogen and oxygen subshells and *independently* refining parameters for both were unproductive because of the high correlations between parameters.

Table II. Restricted Fits to Second-Sphere Fourier-Filtered EXAFS[a]

		shell 2a (C; σ^2 = 40 pm^2)		shell 2b (Fe)			quality of fit		
no.	sample	n	r	n	r	σ^2	R	Δr_{2a}	Δr_{2b}
1T	$Fe(acac)_3$	{5.4 4.2}	{2.95 3.33}				0.20	{0 +20}	
2	$[(TPP)Fe]_2O$	*6.8*	*3.07*	*1*	*3.60*	*71*	*0.48*	*-30*	*+80*
		6.3	3.09	{1 1}	{3.36[b] 3.57}	{37 55}	0.07	-10	{-160 +50}
3	$(HXTA)Fe_2OH(OH_2)_2$	*4.2*	*3.17*				*0.49*		
				1	*3.14*	*61*	*0.48*		*0*
		4.1	2.92	1	3.12	60	0.31	-20	-20
4	$[(HXTA)Fe_2O(OH)]_2^{4-}$	*3.2*	*3.50*	*2*	*2.92*	*267*	*0.11*		
		1.5	2.96	2	3.46	173	0.17	-20	+10
5	$[(HB(pz)_3)Fe]_2OH(OAc)_2^+$			*1*	*3.01*	*68*	*0.50*		
				1	*3.43*	*77*	*0.57*		*-10*
		4.3	*3.47*	*1*	*3.01*	*75*	*0.33*		
		4.4	3.04	1	3.44	80	0.32	+20	0
6	$[(HB(pz)_3)Fe]_2O(OAc)_2$	*8.5*	*3.16*				*0.45*		
				1	3.14	41	0.25		-10
		1.8	3.03	1	3.14	34	0.22	-30	-10
8	$[(tacn)Fe]_2O(OAc)_2^{2+}$			*1*	*3.02*	*51*	*0.31*		-40
		5.0	2.99	1	3.05	57	0.16	-10	-10
9	$[(Me_3tacn)Fe]_2OH(OAc)_2^+$	*2.5*	*3.09*				*0.14*		
		3.2	3.09	1	3.30	230	0.11		-20

[a] Back-transform limits are 2.4–3.4 Å. Various one-, two-, and three-shell fits are shown. For shell 2a (carbon), n is refined, whereas σ^2 is refined for shell 2b (iron). Numbers in italics indicate fits rejected because of higher R or because $r_{2a} > 3.2$ Å, which is considered physically unreasonable (see the text). The Δr values are defined as in Table I. [b] The short (3.37-Å) Fe–Fe distance refined in the three-shell fit for **2** is due to multiple-scattering pathways involving the oxo bridge. Such multiple scattering is expected to cause an apparent shortening of the Fe–Fe distance by 0.2 Å.[34] The single-scattering EXAFS is apparently also observed as the 3.57-Å Fe–Fe distance.

Table III. Distances Obtained by Multishell Restricted Fits to EXAFS Data of Protein Samples

	shell, r in Å					
sample	1s (1 O)	1 (O/N)[a]	2a (C, n)	2b (1 Fe)	3 (C, n)	R
model cmpd **6**	1.788	2.123	3.068 (3.8)	3.155	4.337 (5.0)	0.43
$metHrN_3$	1.801	2.128	3.049 (4.2)	3.188	4.333 (5.1)	1.11
$semimetHrN_3$[b]	1.869[b]	2.135	3.167 (3.1)	3.457	4.337 (4.3)	1.05
RRB_2	1.795	2.062	3.033 (3.1)	3.218	4.299 (3.8)	1.64
RRB_2 + hydroxyurea	1.782	2.060	2.994 (5.7)	3.191	4.30 (4.0)	1.66

[a] Shell 1 modeled as 2 O and 3 N, as described in Table I. [b] $SemimetHrN_3$ is modeled as 0.5 O (per iron) in shell 1s and 2.5 O and 3 N in shell 1.

shell at about 3 Å (shell 2a, which in some cases also models iron–nitrogen interactions) and the iron–iron interaction (shell 2b). The values of A (0.44), σ^2 (40 pm^2), and ΔE (0 eV) for second-sphere iron–carbon distances were determined from the EXAFS of $Fe(acac)_3$.[37] We elected to refine n rather than σ^2 for carbon atoms, because n is not known in the protein samples (nor in some of our model compounds, since it is not always obvious how to cluster the various interatomic distances into shells). On the other hand, the number of iron–iron distances is known (usually one) in our model compounds and proteins. Thus, in this case the disorder factor is refined. Values of A (0.77) and ΔE (−5 eV) for an iron scatterer were determined by analyzing the second-sphere difference spectrum between **6** and **5**.[38]

Various single-shell and two-shell restricted fits of the second-sphere Fourier-filtered data are shown in Table II. Though we are primarily interested in the iron–iron distance, inclusion of a carbon shell at 3.0 Å in the structural model gives more accurate r_{Fe-Fe} values, even where no distinct peaks are seen in the Fourier transform (as in compounds **8** and **9**). Alternative models with $r_{Fe-C} > 3.2$ Å (cf. compounds **4** and **5**) were rejected, because such three bond Fe–C distances are expected to have high σ^2 values.

In all model complexes except **2**, single-scattering theory successfully predicts interatomic distances (±0.02 Å) for two shells of scatterers.[39] The exception, $[(TPP)Fe]_2O$, has a 174° Fe–O–Fe angle about the μ-oxo bridge. Particularly with angles greater than ca. 150°, multiple scattering can cause single-scattering theory (eq 1) to fail.[40,41]

Third Coordination Sphere. The 4- and 5-carbon atoms of the pyrazole rings of the $HB(pz)_3$ ligand are about 4.3 Å from the iron atom and are nearly collinear with the Fe–N bond (∠Fe–N–C = 155–170°). Similarly, the methyl carbon atoms in bridging acetate groups in **5**–**7**, and **9** are also 4.3 Å from the iron with an intervening oxygen (∠Fe–O–C = 160–170°). With angles larger than 150°, multiple scattering increases (up to ninefold, theoretically) the EXAFS amplitude [$f(k)$] and changes the phase relations [$\alpha(k)$] found in eq 5.[40,41] The equations Teo devised to analyze such multiple scattering cannot be used for compounds with unknown coordination (i.e., ribonucleotide reductase) because

(37) Because of the small σ^2 values obtained when the BFBT value of $A \approx 0.3$ was used, we elected to use the same value of A as used for the first-sphere scatterers ($A = 0.44$). The values of σ^2 and ΔE were chosen so as to give the most accurate values of n and r for the two carbon shells of both data sets for **1** (see Table II).

(38) Other than the iron–iron distance, **5** and **6** have similar second coordination spheres (Figure S3), and thus the EXAFS contributions from low Z scatterers largely cancel in the difference spectrum when back-transform limits of 2.4–3.5 Å are used. A two-shell fit gave $R = 0.09$, $A = 0.77$, $\Delta E = -4.3$ eV; shell 1 (N = +1, positive contribution from **6**), $r = 3.15$ Å, $\sigma^2 = 0.0018$ Å^2; shell 2 (N = −1, due to subtraction of EXAFS of **5**), $r = 3.45$ Å, $\sigma^2 = 0.0075$ Å^2. The value of A for restricted fits was taken from this refinement, and ΔE was set to −5 eV to make the refined distances for the difference spectrum virtually identical with the crystallographic iron–iron distances.

(39) By assuming A and ΔE to be equal for Fe–P and Fe–Fe interactions, and with σ^2(Fe–P) = 40 pm^2, a satisfactory two-shell (Fe–P and Fe–Fe) fit to **7** was obtained. However, these assumptions need to be verified or altered based on other model compounds with phosphorus in the second coordination sphere of iron.

(40) Teo, B. K. *J. Am. Chem. Soc.* **1981**, *103*, 3990–4001.
(41) Co, M. S.; Hendrickson, W. A.; Hodgson, K. O.; Doniach, S. *J. Am. Chem. Soc.* **1983**, *105*, 1144–1150.

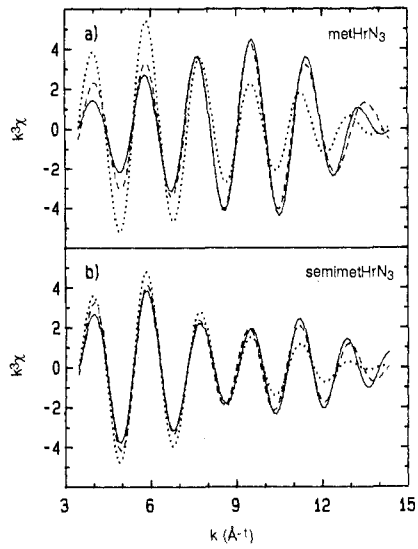

Figure 4. One- (···) and two- (- -) shell restricted fits to the Fourier-filtered (back-transform 1.1–2.3 Å) EXAFS spectra (—) of metHrN$_3$ and semimetHrN$_3$.

of correlations between the many parameters.[40] For simplicity we have made the crude assumptions that the pathways and angles for multiple scattering involving the third coordination sphere are similar in the model compounds and proteins and have continued to use eq 5 to analyze the third-sphere EXAFS. Thus, our treatment of the third coordination sphere is identical with that of the inner spheres, where the single-scattering formalism is more theoretically justified. Restricted fits of third-sphere parameters were made possible by determining A (0.8), σ^2 (60 pm^2), and ΔE (−22 eV) with the model compounds **5** and **6**.[42] The increase in the amplitude due to multiple scattering results in a larger value of A, and the change in the phase function results in significant decrease in ΔE.

Multishell Restricted Fits. Contributions to the EXAFS spectrum from base-line error, first sphere, second sphere, and third sphere overlap in the Fourier transform, so that parameters from a given sphere are somewhat correlated with parameters in other coordination spheres. We report in Table S3 and graphically in Figures S2 and S3 (supplementary material) refined parameters from multishell restricted fits of the unfiltered EXAFS. In these refinements, the cubic-spline parameters for the base line were refined simultaneously.[31] We have the highest confidence in these multishell fits, because they are not biased by subjective choices of base-line correction and Fourier transform windows. However, in nearly all cases, the multishell refinements give results insignificantly different from those on Fourier-filtered data.

The differences between crystallographic (assumed accurate) and EXAFS interatomic distances provide a measure of the accuracy of the EXAFS results. These esd's (Table S3) are ca. 0.015, 0.02, and 0.03 Å for distances from the first, second, and third coordination spheres, respectively.[43]

Methemerythrin Azide. As shown in Figures 2 and 3, the EXAFS spectrum of metHrN$_3$ and its Fourier transform are very similar to those of [(HB(pz)$_3$)Fe]$_2$O(OAc)$_2$ (**6**). The similarity persists in first-sphere and multishell analyses (Tables I and S3). Inclusion of the μ-oxo bridge as a separate shell is clearly justified by the improvement in fit shown in Figure 4. The refined bond lengths of metHrN$_3$ and **6** are virtually identical, with the possible exception of the iron–iron distance, which is longer in the protein than in the model compound by two esd's. The refined disorder factors σ^2 are smaller in the protein than in the model. This may be due in part to the lower temperature (77 K) used for the frozen protein samples. The negative values for σ^2_{1s} for the protein samples may be due in part to problems in $a(E)$ used in converting A_{exp} to χ (see Table S1); in this case the refined σ^2 values for all shells would be too low. The *relative* values of the disorder parameters ($\sigma^2_{1s} < \sigma^2_1 < \sigma^2_{2b}$) reflect the small vibrational disorder of the strong Fe–μ-oxo bond and the much larger (because there is no direct bonding) vibrational motion of the Fe–Fe distance.

The bond lengths for metHrN$_3$ obtained by our EXAFS analysis are similar to those obtained in previous EXAFS studies[44,45] and in the most recent published crystallographic characterization.[33] The determined short Fe–O bond length falls within 1.78 ± 0.02 Å. A disagreement between EXAFS and crystallographic analyses occurs for the longer Fe–O/N bonds, which average 2.24 Å in the crystallographic refinement, 0.1 Å longer than in the present and two previous (2.10[44] and 2.15[45] Å) EXAFS studies. On the other hand, the present EXAFS gives a Fe–Fe distance closer to the crystallographically determined value (3.25 Å) than those determined by the two initial EXAFS studies (3.38[44] and 3.49[45] Å). The longer Fe–Fe distance in one of these early EXAFS studies resulted from the assumption that multiple scattering involving the Fe–Fe distance is important in metHrN$_3$.[44,43] As discussed above, multiple scattering is apparently unimportant in the hemerythrin-like model compounds and so is unlikely to play a role in metHrN$_3$. This same conclusion was reached recently by Hodgson and co-workers based on their own study of compounds **5–8**, and they now favor the 3.20 Å Fe–Fe distance obtained from their metHrN$_3$ data when multiple scattering is neglected.[34]

Semimethemerythrin Azide. The one-electron reduced iron center in semimethemerythrins contain one Fe^{3+} and one Fe^{2+}. Since the empirical parameters A and ΔE were determined with ferric model compounds, the "restricted fit" protocol is not a priori applicable to compounds with iron in other oxidation states. We have applied the restricted fit analysis to **9**, a diferrous model for deoxyhemerythrin. The match between refined EXAFS and crystallographic distances is not as good for this compound as for the iron(III) compounds; errors in the Fe–O/N bond lengths and the Fe–Fe distance are +0.03 and −0.03 Å (Table S3). Thus, average bond lengths and distances obtained for semimetHrN$_3$ are somewhat more uncertain than those for the other proteins.

Figure 4 compares the first-sphere Fourier-filtered EXAFS for met- and semimetHrN$_3$. The differences strongly suggest that the μ-oxo bridge of metHrN$_3$ is either protonated or broken in the one-electron reduced form. For metHrN$_3$, RRB$_2$, and model compounds with μ-oxo groups (data not shown), the amplitudes of the $k^3\chi$ oscillations are largest near k = 10 Å^{-1}. In contrast, a theoretical one-shell fit gives maximum amplitude at k = 6 Å^{-1}. This is observed in the EXAFS of semimetHrN$_3$ as well as for model compounds **1** and **5**. As shown in Figure 4 and Table I, a single-shell calculation gives a much better fit for the semimetHrN$_3$ data than for the metHrN$_3$ data. This indicates that the 1.80-Å Fe–μ-O bonds in metHrN$_3$ have either lengthened or become much more disordered in semimetHrN$_3$, so that inclusion of shell 1s is less important for achieving a good fit. The refined one-shell distance of 2.14 Å is not significantly different between the two forms of hemerythrin.

The R value obtained from the one-shell first-sphere fit to the EXAFS of semimetHrN$_3$ is similar to that for fits deemed satisfactory for model complexes **1–3**. However, this value can be halved by adding a short Fe–O for semimetHrN$_3$. This two-shell fit is visually more satisfactory than the single-shell fit, because the former predicts the slight increase in amplitude at k = 12 Å^{-1} (see Figure 4). The longer refined r_{1s} (1.87 Å) in semimetHrN$_3$ means that shells 1s and 1 are not as well separated as in met-

(42) We assume that the dominant contribution to the third-sphere EXAFS of **5** and **6** arises from the pyrazole carbons. The crystallographic distances were used to set ΔE, and A and σ^2 were adjusted to give fits with accurate distances and $n_3 \approx 6$.

(43) Standard deviations of the refined distances, estimated from the variance/covariance matrix of the least-squares refinement on unfiltered data changed over a twofold range from sample to sample (depending largely on the quality of the data) but averaged 0.005, 0.010, and 0.02 Å for the three spheres.

(44) Hendrickson, W. A.; Co, M. S.; Smith, J. L.; Hodgson, K. O.; Klippenstein, G. L. *Proc. Natl. Acad. Sci. U.S.A.* **1982**, *79*, 6255–6259.

(45) Elam, W. T.; Stern, E. A.; McCalum, J. D.; Sanders-Loehr, J. *J. Am. Chem. Soc.* **1982**, *104*, 6369–6373.

hemerythrin azide, which explains why the single-shell fit is marginally satisfactory only for semimetHrN$_3$. The fit with $n_{1s} = 1$, corresponding to a short oxygen bound to each of the iron atoms, results in $\sigma_{1s}^2 > \sigma_1^2$, which we consider unlikely since shorter bonds are expected to have less vibrational motion. A restricted fit with $\sigma_{1s}^2 < \sigma_1^2$ is obtained with a short oxygen bond included for only one of the iron atoms, implying that the iron centers are asymetrically bridged. Such an asymmetric bridge with the shorter bond to the Fe(III) would be consistent with the mixed-valence nature of the complex, and this is the model we prefer.

The binuclear iron center in semimetHrN$_3$ is known to contain localized high-spin iron(III) and iron(II) centers, which are weakly antiferromagnetically coupled ($-J \approx 20$ cm^{-1}).[9] The smaller value of $-J$ compared with that for methemerythrins ($-J \approx 100$ cm^{-1})[3] could be due to (i) diminished effectiveness of an oxo bridge in mediating coupling between Fe(II) and Fe(III), (ii) protonation of the oxo group to give a μ-hydroxo bridge; or (iii) lack of bridging ligands other than the O,O-bridging carboxylates found in both met and oxy forms of Hr. The last possibility is ruled out because carboxylates alone would be expected to result in $-J < 4$ cm^{-1}.[46] An example of an oxo-bridged Fe(III)–Fe(II) complex has recently been prepared as an aggregate with sodium ions: {Na[Fe(acacen)]$_2$O}$_2$.[47] The complex exhibits Fe–μ-O bond lengths of 2.00 and 2.07 Å and a magnetic moment of 3.64 μ_B at 290 K, which corresponds to $-J \approx 30$ cm^{-1}.[48] The significantly longer Fe–O bonds (relative to Fe(III)–oxo bonds) and, consequently, the diminished value for $-J$ (relative to the value of ca. 100 cm^{-1} for μ-oxo-diiron(III) complexes[49]) are presumably due to the coordination of sodium ion to the oxo group. Protonation of the oxo group would seem to have the same effect as sodium coordination. Although there are as yet no examples of μ-hydroxo-bridged Fe(III)–Fe(II) complexes, both hydroxo-bridged diferric and diferrous complexes are known, e.g., **3**, **5**, and **9**. Based on these complexes, bond lengths for Fe(III)–OH and Fe(II)–OH are ca. 1.96 and 1.99 Å, respectively, and $-J$ values are in the 10–20 cm^{-1} range.[14,15,18,50] The similarity in J between the synthetic hydroxo-bridged dimers and semimetHrN$_3$ ($-J = 20 \pm 3$ cm^{-1}),[9] as well as the absence of an Fe–O–Fe stretch in the resonance Raman spectrum of semimetHrN$_3$,[8] previously led us to propose that semimetHrN$_3$ is hydroxo bridged.[9]

The refined Fe–O distance (1.87 Å) for semimetHrN$_3$ based on the two-shell fit is halfway between the bond distances of diferric model complexes containing a μ-oxo bridge (i.e., **6**, 1.78 Å) and those containing a μ-hydroxo bridge (i.e., **5**, 1.96 Å). On the basis of charge arguments, reduction of an Fe(III)–X–Fe(III) unit to a *localized* Fe(III)–X–Fe(II) unit should shorten the remaining Fe(III)–X bond length. Thus, the observed bond length would suggest that the μ-oxo bridge in metHrN$_3$ becomes protonated in semimetHrN$_3$.

The iron–iron separation in semimetHrN$_3$ lengthens relative to that in metHrN$_3$, in response to the lengthening of the Fe–μ-oxo bonds. The iron–iron distance (3.46 Å) is very similar to that in hydroxo-diacetato-bridged **5** and suggests that the carboxylate bridges remain intact in semimetHrN$_3$. The iron–iron separation is longer by 0.14 Å than that in **9** We suspect that the relatively short Fe–Fe distance (3.32 Å) in **9** is not a function of oxidation state but rather is related to the small ∠N–Fe–N angle required by the Me$_3$tacn ligand; this is analogous to the shorter Fe–Fe separations in the oxo-bridged complexes of tacn (i.e., **8**) compared with those of HB(pz)$_3$ (i.e., **6**).

The average bond length for the remaining ligands of semimetHrN$_3$ [excluding the hydroxo(oxo) bridge] is only 0.01 Å longer than that for the non-oxo bonds in metHrN$_3$ despite the reduction of the binuclear center. Although the ionic radius of 6-coordinate high-spin iron is 0.135 Å shorter for the ferric ion than for the ferrous ion,[51] the small change in average bond length between semimetHrN$_3$ and metHrN$_3$ can be understood by assuming a hydroxo bridge in semimetHrN$_3$. The average bond length for the non-oxo ligands in the hydroxo-bridged diferrous complex **9** is 0.06 Å longer than that in the oxo-bridged diferric complex [(Me$_3$tacn)Fe]$_2$O(OAc)$_2^{2+}$;[18] a similar lengthening of the iron(II) bond lengths in semimetHrN$_3$ relative to the same bonds in metHrN$_3$ is expected (assuming a hydroxo bridge in semimetHrN$_3$). However, the five long bonds/iron in **6** shorten by 0.06 Å upon protonation of the μ-oxo bridge to give **5**; protonation of the μ-oxo bridge upon one-electron reduction of metHrN$_3$ should cause a similar shortening of the bond lengths to the iron, which remains oxidized in semimetHrN$_3$. Since EXAFS analysis cannot resolve the iron(III) and iron(II) bonds, the lengthened bonds of the iron(II) ligands are offset by the shortened bonds of the iron(III) ligands in semimetHrN$_3$ to give the same average bond length (excluding the short Fe–O bond) as that observed in metHrN$_3$. Taken together, the EXAFS data suggest that the binuclear cluster in semimetHrN$_3$ retains most of the structural features of the cluster in metHrN$_3$, except that the oxo bridge becomes protonated.

B$_2$ Subunit of Ribonucleotide Reductase. The EXAFS of RRB$_2$ is very similar when the sample is prepared with or without hydroxyurea, which reduces the tyrosyl radical. The first-shell analysis of RRB$_2$, like that of metHrN$_3$, clearly shows the presence of a 1.78 ± 0.02-Å Fe–O bond, indicative of the Fe–O–Fe bridge previously identified in RRB$_2$ by resonance Raman spectroscopy.[6] The Fourier transform of RRB$_2$ differs from metHrN$_3$ most conspicuously in the size of the peak at $r' = 1.3$ Å. This appears to be related to the very negative σ_{1s}^2 (Table I), which is more negative than that refined for the hemerythrins or the model complexes. A possible explanation for the larger $r' = 1.3$ Å peak is that there are two oxo bridges in RRB$_2$ or, in any case, two short Fe–O bonds/iron, which comprise shell 1s. This was tested as shown in Table I and rejected on the basis of the threefold larger R observed. The similar 3.2-Å refined Fe–Fe distances for RRB$_2$ and metHrN$_3$ suggest there are two carboxylate bridges as well as an oxo bridge in ribonucleotide reductase. This is also suggested by spectroscopic similarities in the visible and Mössbauer spectra and in enhancement profiles for the resonance Raman ν_s (Fe–O–Fe) band at ca. 500 cm^{-1}.[5,6,52]

The number of nitrogen ligands to iron in RRB$_2$ is unknown, as is the overall coordination number. Figure S4 (supplementary material) shows the variation in refined bond length with nitrogen content of shell 1 (containing a total of 5 O/N atoms/iron). The refined average distance is 2.06 ± 0.01 Å for shell 1 of RRB$_2$ as long as at least one of the ligands on each iron is nitrogenous. This appears to be the case, based on observation of a solvent exchangeable ^{1}H NMR resonance at 24 ppm characteristic of histidine ligated to the antiferromagnetically coupled binuclear iron center;[53] the scatterers at 4.3 Å in the EXAFS analysis are consistent with histidine coordination. For all tabulated restricted fits, three nitrogen ligands/iron are assumed for shell 1, as in metHrN$_3$.

The EXAFS-determined interatomic distances between metHrN$_3$ and RRB$_2$ differ principally for shell 1, which consists of all bonds except the Fe–(μ-oxo) bond. These bonds are on average 0.07 Å shorter in RRB$_2$. This difference by 5 esd's is much greater than the effects of the nitrogen/oxygen ratio (Figure S4). Diferric complexes with the (μ-oxo)bis(μ-carboxylato or -phosphatato) core and three nonbridging nitrogen ligands/iron have average bond lengths (excluding Fe–μ-O) of 2.12 ± 0.01 Å by EXAFS (Figure S2) and/or crystallography (excepting the crystal structure of MetHrN$_3$). Thus, if RRB$_2$ does contain the triply bridged hemerythrin core, the shortening of the average bond

(46) Reem, R. C.; Solomon, E. I. *J. Am. Chem. Soc.* **1984**, *106*, 8323–8325.
(47) Arena, F.; Floriani, C.; Chiesi-Villa, A.; Guastini, C. *J. Chem. Soc., Chem. Commun.* **1986**, 1369–1371.
(48) Calculated for the coupling of $S = 2$ and $S = {}^5/_2$ centers by using equations from: Wojciechowski, W. *Inorg. Chim. Acta* **1967**, *1*, 324–328.
(49) Murray, K. S. *Coord. Chem. Rev.* **1967**, *1*, 324–328.
(50) Murch, B. P. Ph.D. Thesis, Cornell University, 1987.
(51) Shannon, R. D. *Acta Crystallogr. A: Cryst. Phys. Diffr. Theor. Gen. Crystallogr.* **1976**, *A32*, 751–767.
(52) Atkin, C. L.; Thelander, L.; Reichard, P.; Lang, G. *J. Biol. Chem.* **1973**, *248*, 7464–7472.
(53) Sahlin, M.; Ehrenberg, A.; Graslund, A.; Sjöberg, B. M. *J. Biol. Chem.* **1986**, *261*, 2778–2780.

length in RRB_2 suggests some of the terminal coordination sites are occupied by oxyanion ligands, which would tend to have shorter bond lengths than neutral nitrogen (i.e., histidine) ligands. Recent resonance Raman investigations implicate hydroxide as a nonbridging ligand of iron in ribonucleotide reductase.[54]

The reduction of the tyrosyl radical of the RRB_2 by addition of hydroxyurea does not cause significant change in the refined interatomic distances. This suggests that any coordination changes accompanying reduction of the radical are minor.

Note Added in Proof. A recently published paper[58] analyzes the EXAFS spectrum of RRB_2 over an energy range (k = 3–9 $Å^{-1}$) smaller than reported here. The two analyses give virtually identical Fe–O and Fe–O/N bond lengths, but they differ in the interpretation of the iron–iron separation. Bunker et al. calculate a 3.26-Å Fe–Fe separation using eq 1, but they claim the actual separation may be as great as 3.48 Å based on singly bridged μ-oxo–diiron complexes where multiple scattering causes Fe–Fe distances so calculated to be as much as 0.22 Å short. In response, we note that, in these cases where multiple scattering is dominant, the Fe–Fe distance appears to be twice the Fe–O bond length minus a phase shift factor of 0.22 Å—namely 3.34 to 3.36 Å.[41] The Fe–Fe distance for RRB_2 determined by us and the 3.26 Å distance of Bunker et al. are 0.1 Å too short to represent artifacts of multiple scattering. Thus we affirm the accuracy of our calculation of a 3.22 ± 0.02 Å Fe–Fe distance and its similarity to the Fe–Fe separation of $metHrN_3$.

Biochemical Implications

A comparison of the EXAFS results for met- and semimethemerythrin azide reveals structural differences between these forms, which differ by one electron in the oxidation state of the diiron center. The 1.80-Å Fe–μ-O bonds and the 3.2-Å Fe–Fe separation of diferric $metHrN_3$ are substantially longer in the mixed-valent [Fe(II)–Fe(III)] protein. This is consistent with the oxygen bridge being protonated in $semimetHrN_3$ and can be interpreted in the context of the proposed mechanism for reversible oxygenation by hemerythrin.[55] In this mechanism, the proton associated with the hydroxo-bridged binuclear unit in deoxyHr is transferred to dioxygen in oxyHr; the hydroxo bridge thus becomes an oxo bridge, and the dioxygen is transformed into a coordinated hydroperoxide. Since dioxygen is coordinated to only one iron in oxyHr, reduction of dioxygen may occur in two one-electron steps, via a putative semimetHr superoxide species.[56] If the structure of such a complex were analogous to that of $semimetHrN_3$, the oxygen bridge would still be protonated at this stage, and proton transfer to the bound dioxygen would occur concomitant with the second electron transfer.[9] Given the energetics of dioxygen reduction,[57] the involvement of a proton would facilitate the superoxide–peroxide interconversion and promote reversible dioxygen binding.

The EXAFS data suggest that the B_2 subunit of ribonucleotide reductase and methemerythrin azide share the (μ-oxo)bis(μ-carboxylato)diiron core. We speculate that this similarity is a consequence of the function of RRB_2 to generate the tyrosyl radical. While the active site of hemerythrin has evolved to reversibly bind dioxygen, the active site of RRB_2 may have evolved to utilize the oxidizing potential of a diferric peroxide complex for generating the tyrosine radical. Thus, in the reactivation of RRB_2 from apoprotein, Fe(II) and O_2,[2] a deoxyHr-like complex may form initially. This then binds O_2 and forms an oxyHr-like complex, which functions as the oxidizing agent for the tyrosine. The greater proportion of oxyanion ligation about iron in ribonucleotide reductase compared with hemerythrin (as suggested by EXAFS bond lengths) may be important for the differing functions of the two proteins.

Acknowledgment. This work was supported by the National Science Foundation (Grant DMB-8314935, L.Q.) and the National Institutes of Health (Grant GM-29595, J.S.). The Cornell High Energy Synchrotron Source is supported by NSF Grant DMR-8412465. R.C.S. is grateful for postdoctoral fellowship support from the NIH and the American Cancer Society. L.Q. is an Alfred P. Sloan Research Fellow and an NIH Research Career Development Awardee. S.P.S. acknowledges a predoctoral fellowship from the NSF. J.S. is an H. I. Romnes Fellow from the University of Wisconsin—Madison and an NIH Research Career Development Awardee. We thank Profs. S. J. Lippard and Karl Wieghardt for their generous gifts of compounds **7–9**. We are also grateful to Prof. D. M. Kurtz for performing the EPR integrations on our samples.

Supplementary Material Available: Tables of EXAFS data analyses (Tables S1–S3) and graphic presentations (Figures S1–S4) (10 pages). Ordering information is given on any current masthead page.

(54) Sjöberg, B.-M.; Sanders-Loehr, J.; Loehr, T. M. *Biochemistry* **1987**, *26*, 4242–4247.
(55) Stenkamp, R. E.; Sieker, L. C.; Jensen, L. H.; McCallum, J. D.; Sanders-Loehr, J. *Proc. Natl. Acad. Sci. U.S.A.* **1985**, *82*, 713–716.
(56) Nocek, J. M.; Kurtz, D. M., Jr.; Sage, J. T.; Debrunner, P. G.; Maroney, M. J.; Que, L., Jr. *J. Am. Chem. Soc.* **1985**, *107*, 3382–3384.
(57) Fee, J. A.; Valentine, J. S. In *Superoxide and Superoxide Dismutases*; Michelson, A. M., McCord, J. M., Fridovich, I., Eds.; Academic: New York, 1977; pp 19–60.
(58) Bunker, G.; Petersson, L.; Sjöberg, B.-M.; Sahlin, M.; Chance, M.; Chance, B.; Ehrenberg, A. *Biochemistry* **1987**, *26*, 4708–4716.